Polyfluorene Terpolymers Containing Phenothiazine and Fluorenone: Effects of Donor and Acceptor Moieties on Energy and Intrachain Charge Transfer Processes in the Photoluminescence and Electroluminescence of Multichromophore Copolymers

Abhishek P. Kulkarni, Xiangxing Kong, and Samson A. Jenekhe*

Department of Chemical Engineering and Department of Chemistry, University of Washington, Seattle, Washington 98195-1750

Received July 26, 2006; Revised Manuscript Received September 29, 2006

ABSTRACT: Five new conjugated terpolymers containing 9,9-dihexylfluorene, 10-hexylphenothiazine (HPT) donor, and 9-fluorenone (FLO) acceptor were synthesized by Suzuki copolymerization and used to study the effects of competing energy and intramolecular charge transfer processes on the photoluminescence (PL) and electroluminescence (EL) of multichromophore copolymers. The HPT and FLO moieties were found to act as emissive exciton traps on the terpolymer chains, leading new blue-green (475−485 nm) and green (520−525 nm) emission bands in addition to the blue (415 nm) emission of the fluorene segments. Additional charge transfer excited states and associated nonradiative decay channels resulting in factors of 2−4 decrease in the solution PL quantum yields of the terpolymers emerged due to the HPT moieties. As the emissive materials in light-emitting diodes (LEDs), the terpolymers showed green to yellow EL with luminances of 1900−8970 cd/m^2 and efficiencies of 0.5−3.5 cd/A that varied with terpolymer composition. As a result of charge trapping within the HPT and FLO moieties, the EL spectra were very sensitive to the applied voltage, the terpolymer composition, and device architecture. These results highlight the complex excited-state dynamics encountered upon incorporation of electron-donating and -accepting moieties in polyfluorenes and have implications for the design of multichromophore EL copolymers for white LEDs.

Introduction

Emissive semiconducting π-conjugated polymers are being extensively investigated as the active elements in organic light-emitting diodes (OLEDs) for applications in full-color displays and lighting.[1,2] To meet the need for balanced hole (p-type) and electron (n-type) transport properties in a single polymer, which is essential to achieving efficient single-layer OLEDs, a common strategy is the incorporation of electron donor (D) and acceptor (A) comonomer units on an otherwise unipolar polymer backbone.[1d] Introduction of such a D−A chain structure generally, but not always, leads to significant changes in the electronic structure of the parent homopolymers, polyD and polyA, often resulting in shifts in the emission color, which may or may not be desirable. Additionally, by acting as exciton and/or charge carrier traps, the D or A moieties can adversely affect the efficiency of energy and charge transfer processes[3] and decrease the photoluminescence (PL) and electroluminescence (EL) efficiencies of the resultant copolymers. This makes it challenging to design optimum copolymers with balanced hole/electron transport properties while still retaining the high solid-state PL quantum yields essential to efficient OLED performance. It is necessary to understand this interplay between D/A copolymer chain structure and the optical and electronic properties to fully exploit the advantages of the copolymerization strategy. From a fundamental standpoint, it is important to develop a clear understanding of the often complex excited-state dynamics encountered in such multicomponent conjugated copolymer systems.[1d,3]

Polyfluorenes (PFs) are currently the most widely studied class of electroluminescent polymers due in part to their attractive blue light emission, high PL quantum yields in the solid state,[4a,b] and easy solution processability.[1,4−8] The parent poly(9,9-dioctylfluorene) (PFO) is a p-type, blue-emitting polymer with a large band gap of ∼3.1 eV, a low electron affinity (EA = 2.5 eV), and a high ionization potential (IP = 5.6 eV),[5c] making it difficult to efficiently inject both electrons and holes into it from the two opposite electrodes in OLEDs. To improve the charge-injection and charge-transport properties (i.e., to lower the IP and increase the EA) of PFO and/or to tune the emission color, PFs have been copolymerized with many D/A moieties, resulting in EL copolymers that emit across the visible spectrum.[4e,5a,b,7,8] The choice of the D/A comonomers and their relative amounts govern the extent of intrachain energy/charge transfer and determine whether the parent blue emission of PF is retained[7] or is red-shifted to green or red colors.[8] Recently, there has been a great interest in developing fluorene-based copolymers for single-layer white OLEDs, where small amounts of green- and orange/red-emitting D/A comonomers are incorporated into the blue-emitting PF backbone.[9] One of the main challenges of this approach to white OLEDs is to obtain voltage-independent EL spectra so as to avoid undesirable shifts in the white emission CIE coordinates with drive voltage. The factors that would lead to a bias-independent white EL are not yet understood; currently, the design of white-emitting copolymers is based on an empirical trial-and-error approach that has met with varying degrees of success.[9] Polyfluorenes and other conjugated copolymers with donor−acceptor architecture have also been of much interest as small band gap polymers with near-infrared absorption for efficient light-harvesting in solar cells[10] and as semiconductors for ambipolar thin film transistors.[11] The copolymer chain architecture, D/A strength, and composition can be expected to critically influence the ground- and excited-state electronic structures and related energy and

* Corresponding author. E-mail: jenekhe@u.washington.edu.

10.1021/ma0617062 CCC: $33.50
Published on Web 11/15/2006

Chart 1

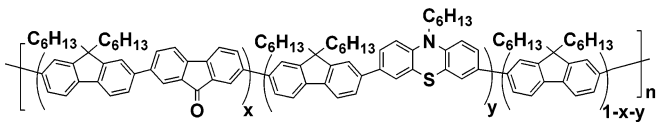

Chart 2

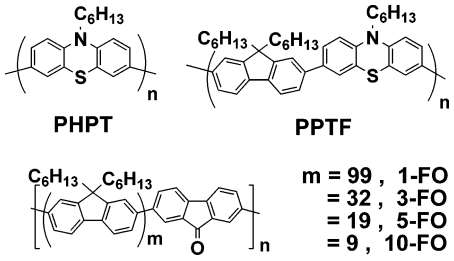

charge transfer dynamics but are not currently well understood in such multichromophore conjugated copolymers.

In this paper, we report studies of the effects of intrachain donor and acceptor moieties on energy and intrachain charge transfer processes that determine the PL and EL of multichromophoric polyfluorenes by using new model polyfluorene terpolymers containing 10-hexylphenothiazine (HPT) and 9-fluorenone (FLO) as the donor and acceptor moieties, respectively. The terpolymers were synthesized by Suzuki coupling polymerization which ensured achievement of well-defined molecular structures (Chart 1). Thus, each HPT or FLO moiety is isolated within the poly(9,9-dihexylfluorene) (PHF) chains, with random distances between them, allowing us to investigate the energy transfer dependence on this distribution in D/A distance. A series of five terpolymers containing 0.5, 1, 2, 4, and 8 mol % each of both HPT and FLO, denoted FOPT-0.5, FOPT-1, FOPT-2, FOPT-4, and FOPT-8 (Chart 1), respectively, were investigated. Our choice of the HPT moiety as the donor stems from prior studies which demonstrated phenothiazine as an excellent donor building block in both emissive D−A small molecules[12a−d] and polymers.[12a,e−g] Our previous studies of two phenothiazine-based polymers, poly(10-hexylphenothiazine-3,7-diyl) (PHPT) and poly(10-hexylphenothiazine-3,7-diyl-*alt*-9,9-dihexyl-2,7-fluorene) (PPTF) whose structures are shown in Chart 2, also demonstrated that phenothiazine effectively lowers the IP of PHF and acts as a good intrachain emissive hole trap.[12e] Fluorenone was chosen as the acceptor on the basis of previous studies, both theoretical[13] and experimental,[14] that showed fluorenone to act as an effective low-energy electron trap on the PF backbone, leading to the green emission band in blue-emitting PFs. Although this has been a highly debated subject in the literature,[4b,13,14] many studies, including ours on the four fluorene−fluorenone copolymers[14d] shown in Chart 2, have now conclusively shown that the green emission originates from the on-chain fluorenone moieties due to efficient intra- and interchain energy transfer and strong localization of the excitons on the fluorenone units.[13,14] Thus, we anticipate competing energy transfer and charge carrier trapping effects upon incorporation of both HPT and FLO moieties on the PHF backbone. Our study aims to gain insights into the complex excited-state dynamics of such D/A terpolymers.

Experimental Section

Materials. 9,9-Dihexyl-2,7-dibromofluorene, 9,9-dihexylfluorene-2,7-bis(trimethylene boronate), Aliquat 336, and tetrakis-(triphenyl)phosphine palladium [$Pd(PPh_3)_4$] were purchased from Aldrich. 10-Hexyl-3,7-bis(4,4,5,5-tetramethyl[1,3,2]dioxaborolan-2-yl)-10*H*-phenothiazine was synthesized from 10-hexyl-3,7-dibromophenothiazine according to a reported procedure.[15]

General Polymerization Procedure for Poly(fluorenone-2,7-diyl-*co*-10-hexylphenothiazin-3,7-diyl-*co*-9,9-dihexyl-2,7-fluorene). In a flask, 9,9-dihexylfluorene-2,7-bis(trimethyleneboronate), 10-hexyl-3,7-bis(4,4,5,5-tetramethyl[1,3,2]dioxaborolan-2-yl)-10*H*-phenothiazine (total 1.0 mmol), 2,7-dibromofluorenone, 2,7-dibromo-9,9-dihexylfluorene (total 1.0 mmol), sodium carbonate (20 mmol, 2.12 g), and 0.05 g of Aliquat 336 were dissolved in a mixture of toluene (15 mL) and water (10 mL) under argon. Pd-$(PPh_3)_4$ (23 mg) was added. The mixture was stirred for 48 h at 100 °C and then washed with water (50 mL). The copolymer was first precipitated into methanol/HCl (100/1, v/v) and purified by precipitation twice from THF solution into methanol/HCl (100/1, v/v).

FOPT-0.5 Terpolymer. The molar ratio among 9,9-dihexylfluorene-2,7-bis(trimethyleneboronate) (497.3 mg, 0.99 mmol), 10-hexyl-3,7-bis(4,4,5,5-tetramethyl[1,3,2]dioxaborolan-2-yl)-10*H*-phenothiazine (5.4 mg, 0.01 mmol), 9,9-dihexyl-2,7-dibromofluorene (487.4 mg, 0.99 mmol), and 2,7-dibromofluorenone (3.4 mg, 0.01 mmol) was 49.5/0.5/49.5/0.5. A light yellow copolymer (0.59 g, 89% yield) was obtained after drying in a vacuum oven at 60 °C. ^{1}H NMR (TMS, $CDCl_3$), δ (ppm): 7.83 (b, Ar−H), 7.66 (b, Ar−H), 2.11 (b, CH_2−fluorene), 1.14, (b, $6CH_2$), 0.79 (b, CH_3, and CH_2). FT-IR (KBr), ν (cm^{-1}): 2954, 2927, 2856, 1457, 812. GPC (THF, PSt standard): $M_n = 1.95 \times 10^4$, $M_w/M_n = 3.28$.

FOPT-1 Terpolymer. The molar ratio among 9,9-dihexylfluorene-2,7-bis(trimethyleneboronate) (492.3 mg, 0.98 mmol), 10-hexyl-3,7-bis(4,4,5,5-tetramethyl[1,3,2]dioxaborolan-2-yl)-10*H*-phenothiazine (10.7 mg, 0.02 mmol), 9,9-dihexyl-2,7-dibromofluorene (482.5 mg, 0.98 mmol), and 2,7-dibromofluorenone (6.8 mg, 0.02 mmol) was 49/1/49/1. A yellow copolymer (0.55 g, 82% yield) was obtained. ^{1}H NMR (TMS, $CDCl_3$), δ (ppm): 7.83 (b, Ar−H), 7.66 (b, Ar−H), 2.11 (b, CH_2−fluorene), 1.14, (b, CH_2), 0.79 (b, CH_3, and CH_2). FT-IR (KBr), ν (cm^{-1}): 2954, 2927, 2856, 1457, 812. GPC (THF, PSt standard): $M_n = 1.60 \times 10^4$, $M_w/M_n = 2.65$.

FOPT-2 Terpolymer. The molar ratio among 9,9-dihexylfluorene-2,7-bis(trimethyleneboronate) (482.2 mg, 0.96 mmol), 10-hexyl-3,7-bis(4,4,5,5-tetramethyl[1,3,2]dioxaborolan-2-yl)-10*H*-phenothiazine (21.4 mg, 0.04 mmol), 9,9-dihexyl-2,7-dibromofluorene (472.6 mg, 0.96 mmol), and 2,7-dibromofluorenone (13.5 mg, 0.04 mmol) was 48/2/48/2. A yellow copolymer (0.60 g, 88% yield) was obtained. ^{1}H NMR (TMS, $CDCl_3$), δ (ppm): 7.83 (b, Ar−H), 7.66 (b, Ar−H), 2.11 (b, CH_2−fluorene), 1.14, (b, CH_2), 0.79 (b, CH_3, and CH_2). FT-IR (KBr), ν (cm^{-1}): 2954, 2927, 2856, 1719 (C═O), 1608, 1457, 813. GPC (THF, PSt standard): $M_n = 2.32 \times 10^4$, $M_w/M_n = 2.98$.

FOPT-4 Terpolymer. The molar ratio among 9,9-dihexylfluorene-2,7-bis(trimethyleneboronate) (462.1 mg, 0.92 mmol), 10-hexyl-3,7-bis(4,4,5,5-tetramethyl[1,3,2]dioxaborolan-2-yl)-10*H*-phenothiazine (42.8 mg, 0.08 mmol), 9,9-dihexyl-2,7-dibromofluorene (452.9 mg, 0.92 mmol), and 2,7-dibromofluorenone (27.0 mg, 0.08 mmol) was 46/4/46/4. A yellow copolymer (0.55 g, 85% yield) was obtained. ^{1}H NMR (TMS, $CDCl_3$), δ (ppm): 8.03 (weak b, Ar−H adjacent to the keto on fluorenone), 7.83 (b, Ar−H), 7.67 (b, Ar−H), 6.99 (b, Ar−H adjacent to nitrogen of phenothiazine), 3.95 (weak b, CH_2 attached to nitrogen of phenothiazine), 2.11 (b, CH_2), 1.14, (b, CH_2), 0.79 (b, CH_3 and CH_2). FT-IR (KBr), ν (cm^{-1}): 2954, 2927, 2856, 1718 (C═O), 1608, 1457, 813. GPC (THF, PSt standard): $M_n = 2.45 \times 10^4$, $M_w/M_n = 2.79$.

FOPT-8 Terpolymer. The molar ratio among 9,9-dihexylfluorene-2,7-bis(trimethyleneboronate) (421.9 mg, 0.84 mmol), 10-hexyl-3,7-bis(4,4,5,5-tetramethyl[1,3,2]dioxaborolan-2-yl)-10*H*-phenothiazine (85.7 mg, 0.16 mmol), 9,9-dihexyl-2,7-dibromofluorene (413.6 mg, 0.84 mmol), and 2,7-dibromofluorenone (54.1 mg, 0.16 mmol) was 42/8/42/8. A brown copolymer (0.54 g, 85% yield) was

Scheme 1

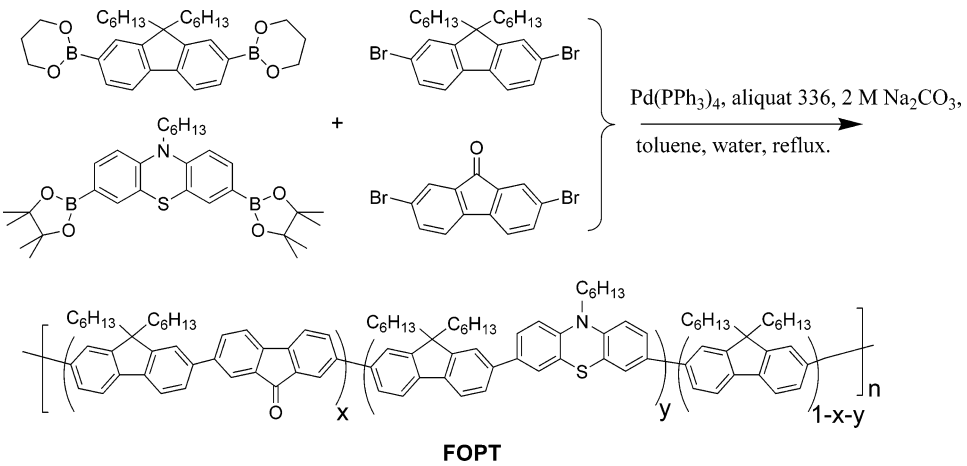

obtained. ^{1}H NMR (TMS, $CDCl_3$), δ (ppm): 8.03 (weak b, Ar−H adjacent to the keto on fluorenone), 7.83 (b, Ar−H), 7.67 (b, Ar−H), 6.99 (b, Ar−H adjacent to nitrogen of phenothiazine), 3.95 (weak b, CH_2 attached to nitrogen of phenothiazine), 2.11 (b, CH_2), 1.14, (b, CH_2), 0.79 (b, CH_3 and CH_2). FT-IR (KBr), ν (cm^{-1}): 2954, 2927, 2856, 1718 (C═O), 1608, 1457, 813. GPC (THF, PSt standard): $M_n = 2.26 \times 10^4$, $M_w/M_n = 2.54$.

Characterization. FT-IR spectra were obtained on a Perkin-Elmer FT-IR 1720 infrared spectrophotometer with KBr pellets. ^{1}H NMR spectra were taken at 300 MHz on a Bruker AV301 spectrometer in chloroform-*d*. GPC analysis of the polymers was done on a Waters GPC with Shodex gel columns and Waters 150 C refractive index detectors at 30 °C with a THF flow rate of 1 mL/min. The molecular weight measurement was calibrated with polystyrene standards.

Optical Absorption and Photoluminescence Spectroscopy. Optical absorption spectra were recorded using a Perkin-Elmer model Lambda 900 UV/vis/near-IR spectrophotometer. Steady-state PL spectra were acquired on a Photon Technology International (PTI) Inc. model QM-2001-4 spectrofluorimeter. Thin films for optical absorption and PL measurements were spin-coated on glass from toluene solutions of polymers. All the films were dried at 60 °C typically overnight in a vacuum to remove any residual solvent. The PL quantum yields of the polymers in solution were estimated by using a 10^{-5} M solution of 9,10-diphenylanthracene in toluene as a standard ($\phi_{PL} = 93\%$).[16]

Time-Resolved Photoluminescence Decay Dynamics. Fluorescence decays were measured on a PTI model QM-2001-4 spectrofluorimeter equipped with Strobe Lifetime upgrade. The instrument utilizes a nanosecond flash lamp as an excitation source and a stroboscopic detection system. The flash lamp was filled with a 30/70 v/v mixture of high-purity nitrogen/helium. All measurements were done at room temperature. The decay curves were analyzed using a multiexponential fitting software provided by the manufacturer. Reduced chi-square values, Durbin−Watson parameters, and weighted residuals were used as the goodness-of-fit criteria.[14d]

Fabrication and Characterization of OLEDs. ITO-coated glass substrates (Delta Technologies Ltd., Stillwater, MN) were cleaned sequentially in ultrasonic bathes of detergent solution, 2-propanol, deionized water, and acetone, and then dried at 60 °C in a vacuum overnight. A 75 nm thick poly(ethylenedioxythiophene)/poly(styrenesulfonate) blend (PEDOT) hole injection layer was spin-coated on top of ITO from a ∼0.75 wt % dispersion in water and dried at 200 °C for 15 min under a vacuum. Before spin-coating, the as-received PEDOT solution was diluted by ∼25% with 1:1 (v/v) water:2-propanol and was then filtered through 0.45 μm PVDF syringe filters. Three types of OLEDs were fabricated with the terpolymers as the emissive material, poly(*N*-vinylcarbazole) (PVK) as the hole-transport/electron-blocking layer and 1,3,5-tris(*N*-phenylbenzimidizol-2-yl)benzene (TPBI) as the electron-transport/hole-blocking layer: (1) ITO/PEDOT/copolymer/LiF/Al, (2) ITO/PEDOT/PVK/copolymer/LiF/Al, and (3) ITO/PEDOT/PVK/copolymer/TPBI/LiF/Al. A 20 nm thick PVK film was obtained by spin-coating on top of PEDOT from its 0.5 wt % solution in toluene and dried in a vacuum at 60 °C overnight. Thin films (40−50 nm) of the copolymers were obtained by spin-coating on top of PEDOT or PVK from 0.8 wt % solutions in toluene and dried in a vacuum at 60 °C overnight. The film thicknesses were measured by an Alpha-Step 500 surface profiler (KLA Tencor, Mountain View, CA) with an accuracy of ±3 nm. Before spin-coating, all the solutions were filtered through 0.2 μm PTFE syringe filters. The underlying PVK layer remained intact due to the low solubility of PVK in toluene. 20 nm thick films of TPBI were obtained by evaporation from resistively heated quartz crucibles at a rate of ∼0.2 nm/s in a vacuum evaporator (Edwards Auto 306) at base pressures of $<7 \times 10^{-7}$ Torr. The chamber was vented with air to load the cathode materials and pumped back down, and then a 2 nm LiF and a 100 nm thick aluminum layer were sequentially deposited through a shadow mask without breaking vacuum to form active diode areas of 0.2 cm^2.

Electroluminescence spectra were obtained using a PTI QM-2001-4 spectrophotometer. Current−voltage characteristics of the LEDs were measured using a HP4155A semiconductor parameter analyzer (Yokogawa Hewlett-Packard, Tokyo). The luminance was simultaneously measured using a model 370 optometer (UDT instruments, Baltimore, MD) equipped with a calibrated luminance sensor head (model 211) and a 5× objective lens. For each device type, two sets of devices were fabricated with a total of 8−10 individual pixel measurements on each copolymer. Although exact averaging was not done, care was taken to report the data where the maximum values were an approximate mean of the 8−10 recorded sample space values. The spread in the maximum brightness values and the maximum drive voltages was found to be within ±10%. The device external quantum efficiencies were calculated using procedures reported previously.[6c,7f] All the device fabrication and characterization steps were done under ambient laboratory conditions.

Results and Discussion

Synthesis and Characterization. The random terpolymers poly(fluorenon-2,7-diyl-*co*-10-hexylphenothiazin-3,7-diyl-*co*-9,9-dihexyl-2,7-fluorene)s containing equimolar fractions of fluorenone (acceptor) and phenothiazine (donor) between 0.5 and 8 mol % were synthesized by Suzuki coupling polymerization (Scheme 1). The molar ratios of fluorenone and phenothiazine in the copolymers were controlled by adjusting the molar ratio between 9,9-dihexyl-2,7-dibromofluorene, 2,7-dibromofluorenone, 9,9-dihexylfluorene-2,7-bis(trimethyleneborate), and 10-hexyl-3,7-bis(4,4,5,5-tetramethyl[1,3,2]dioxaborolan-2-yl)-10*H*-phenothiazine while maintaining a 1/1 molar ratio between the dibromides and the boronate esters. The colors of

Table 1. Molecular Weights of the Terpolymers

terpolymer	fluorenone and phenothiazine fraction (%, mol/mol)	M_n[a] ($\times 10^4$)	M_w/M_n[a]	DP_n[b]
FOPT-0.5	0.5	1.95	3.28	99
FOPT-1	1.0	1.60	2.65	80
FOPT-2	2.0	2.32	2.98	90
FOPT-4	4.0	2.45	2.79	87
FOPT-8	8.0	2.26	2.54	77

[a] Measured by GPC using PSt standards. [b] Degree of polymerization = M_n/MW_{DHF}.

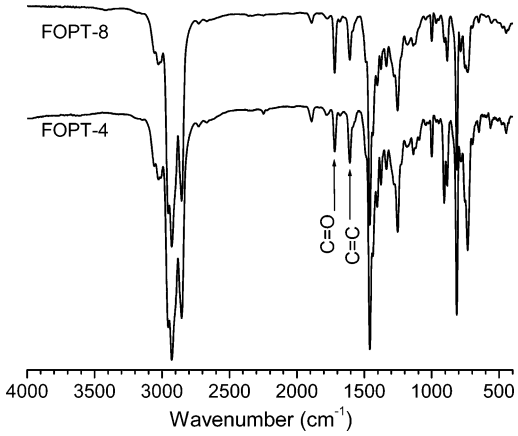

Figure 1. FT-IR spectra of terpolymers FOPT-4 and FOPT-8.

the terpolymers were light yellow for FOPT-0.5 and FOPT-1, yellow for FOPT-2 and FOPT-4, and brown for FOPT-8. All the terpolymers were soluble in organic solvents such as chloroform, toluene, and tetrahydrofuran. The terpolymers have number-average molecular weights (M_n, GPC, polystyrene calibration) between 16 000 and 24 500, as shown in Table 1. The number-average degree of polymerization (DP_n) was in the range 77−99.

Figure 1 shows the FT-IR spectra of two terpolymers FOPT-4 and FOPT-8. Two main vibrational bands located at 1719 and 1448 cm^{-1} are characteristic of the C═O stretch in fluorenone moiety and the aromatic C═C, respectively.[14d] The peak at 1606 cm^{-1} is related to the fluorenone moiety and assigned to a stretching mode of an asymmetrically substituted benzene ring.[14d] With increasing fluorenone amount in the terpolymers, the relative intensity of the keto vibration band at 1719 cm^{-1} increased. The structures of the terpolymers were also confirmed by ^1H NMR spectra. The ^1H NMR spectra of FOPT-4 and FOPT-8 and their assignment, shown in Figure 2, are consistent with the proposed structures. A small peak at 8.03 ppm due to the aromatic proton adjacent to the keto group in fluorenone was observed in the spectra of FOPT-4 and FOPT-8, but not in FOPT-2, FOPT-1, and FOPT-0.5 because of the low concentration of fluorenone. With the increase of the phenothiazine fraction in the terpolymers, two new peaks appeared at 3.95 and 6.99 ppm; the former was assigned to the methylene proton adjacent to the nitrogen in the phenothiazine ring, and the latter was assigned to the aromatic proton in the phenothiazine ring adjacent to the nitrogen atom.[12e]

Steady-State Photophysics. a. Solutions. Figure 3a shows the normalized optical absorption spectra of dilute (10^{-5} M) toluene solutions of PHF homopolymer and the five FOPT terpolymers. The main absorption band progressively blue-shifts from 386 nm in PHF homopolymer to 379 nm in FOPT-8 with increasing fraction of phenothiazine and fluorenone. This band is associated with the $\pi-\pi^*$ transition of the polyfluorene backbone.[4a] A very weak absorption band extending from 430

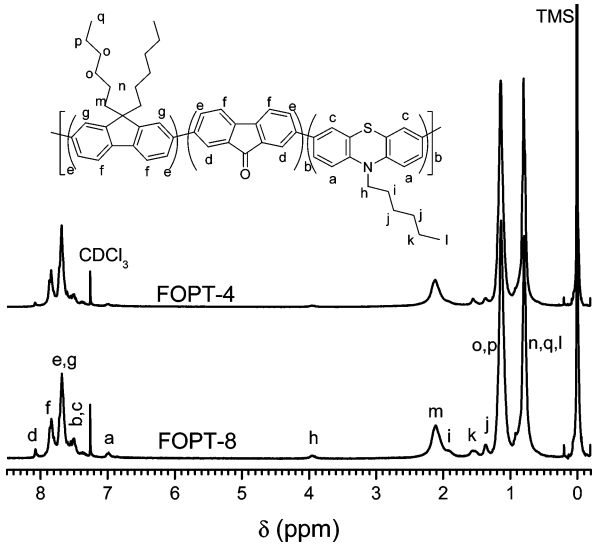

Figure 2. ^1H NMR spectra of terpolymers FOPT-4 and FOPT-8.

to 500 nm is observed in all the FOPT terpolymers; the intensity of this band increases with increasing fluorenone content from FOPT-0.5 to FOPT-8, as shown in the inset of Figure 3a. This broad absorption band is likely related to the intramolecular charge transfer (ICT) transition between fluorene and fluorenone moieties, similar to that observed in fluorene−fluorenone copolymers previously reported.[14d,g] The phenothiazine moiety appears to have no clearly observable modification of the PF absorption band.

Figure 3b shows the photoluminescence (PL) emission spectra of PHF homopolymer, PPTF copolymer, and the five terpolymers in 10^{-6} M toluene solutions, normalized relative to the blue peak. The PL spectrum of PHF shows the typical well-resolved blue emission with peaks at 414 and 437 nm. In addition to these two peaks, the FOPT terpolymers have two other emission features in their PL spectra: a blue-green band centered at 475−485 nm and a green band centered at 520−525 nm. The relative intensity of these two additional bands grows along with a gradual red shift with increasing phenothiazine and fluorenone concentration in the copolymers, finally becoming 1.6 and 2.0 times the intensity of the blue band at 414 nm in FOPT-8. These are thus clearly associated with the phenothiazine and fluorenone moieties on the terpolymer chains. The blue-green emission in the terpolymers is identical to the emission of the alternating phenothiazine−fluorene copolymer PPTF (PL maximum at 485 nm) whose PL spectrum is also shown in Figure 3b. Thus, this emission peak can be assigned to the phenothiazine−fluorene conjugated segments in the terpolymers. Intrachain energy transfer from the high-energy fluorene segments to the low-energy phenothiazine-containing segments is responsible for this emission, given the small concentration of phenothiazine in the terpolymers. In the alternating PPTF copolymer, the blue emission bands (414 and 437 nm) are completely suppressed in dilute solution;[12e] however, in the FOPT terpolymers, the blue emission persists due to the much lower fraction (≤8 mol %) of phenothiazine in them. The green emission (520−525 nm) in the FOPT terpolymers can be assigned to the intramolecular charge transfer (ICT) excited state associated with the on-chain fluorenone moieties.[13a,14g] The intrachain excitation energy transfer from the fluorene segments to the fluorenone-containing segments populates this ICT excited state. This green band is blue-shifted by 10−15 nm relative to the 535 nm band that was previously observed in the fluorene−fluorenone copolymers in toluene

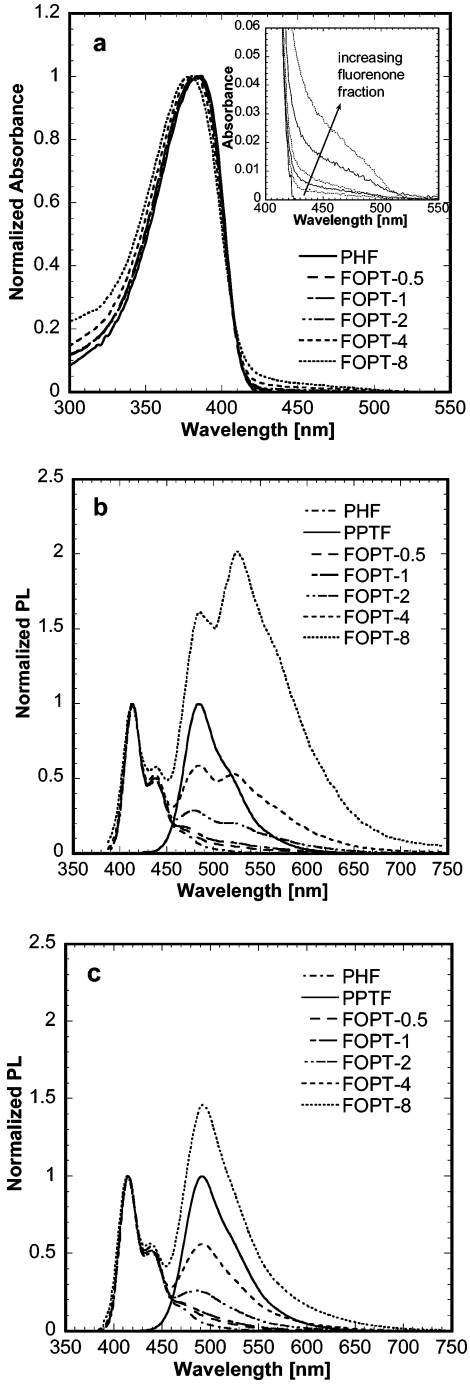

Figure 3. (a) Optical absorption spectra of 10^{-5} M solutions of PHF and the terpolymers in toluene. The inset shows the same absorption spectra on a magnified scale. Normalized PL emission spectra of 10^{-6} M solutions of the polymers in toluene (b) and dichloromethane (c) under 380 nm excitation.

solution.[14d] Three distinct spectral features are thus observed in the PL emission of the FOPT terpolymers upon excitation of the high-energy fluorene segments at 380 nm: (i) the blue emission (414 and 437 nm) from the fluorene segments, (ii) the blue-green emission (475−485 nm) from the phenothiazine-containing segments due to intrachain energy transfer, and (iii) the green charge transfer emission (520−525 nm) from the fluorenone-containing segments arising from intrachain energy transfer from the fluorene segments.

To investigate the effect of the solvent polarity on the charge transfer photophysics of the FOPT terpolymers, their PL emission spectra were also acquired in dichloromethane which has a higher dielectric constant ($\epsilon = 8.93$) compared to toluene ($\epsilon = 2.38$).[17] Figure 3c shows the PL emission spectra of all the polymers in 10^{-6} M dichloromethane solutions, normalized relative to the blue peak. Two blue emission features at 415 and 438 nm associated with the polyfluorene backbone are observed in the FOPT terpolymers. In addition, a blue-green band (485−492 nm) is observed. However, unlike the emission spectra in toluene, the green emission feature (520−525 nm) is absent in all the FOPT terpolymers in dichloromethane. The blue-green emission increases in intensity and progressively red-shifts in going from FOPT-0.5 to FOPT-8. In each terpolymer, the intensity of the blue-green emission band relative to the blue peak is nearly identical in both toluene and dichloromethane; the position of this emission peak is red-shifted by 7−10 nm in the more polar environment of dichloromethane. The alternating copolymer PPTF has an emission maximum at 491 nm in dichloromethane, which is also red-shifted by 6 nm compared to toluene. The observed red shift in the emission band with increase in solvent polarity is due to a small degree of ICT character associated with the excited state delocalized over phenothiazine−fluorene segments. Charge transfer excited states have been observed in alternating fluorene copolymers containing strong electron donors such as triarylamines.[18] Since phenothiazine is a strong electron donor, it is able to form charge transfer states with fluorene as a weak acceptor. In the fluorene−fluorenone pair, fluorenone is a strong electron acceptor and fluorene acts as the electron donor. Fluorene has a much stronger electron-donating character than an electron-accepting character. Thus, the excited-state charge transfer character associated with the phenothiazine−fluorene segments is expected to be much weaker compared to that associated with the fluorenone−fluorene segments. Hence, the blue-green emission from the phenothiazine-containing segments has the same intensity in both dichloromethane and toluene. On the other hand, the green emission (520−525 nm) associated with the fluorenone-containing segments is drastically quenched in the high-polarity environment of dichloromethane. Such dramatic quenching of the green fluorenone emission band in high-polarity solvents has been previously observed in other fluorene−fluorenone copolymers.[14g]

It is well-known that increased excited-state ICT character reduces the PL quantum yield (ϕ_f) of emissive conjugated copolymers.[12a,13a] For example, the PL quantum yield steadily decreased with increasing amount of fluorenone in fluorene−fluorenone copolymers.[14d] The estimated ϕ_f values of the current polymers in 10^{-6} M toluene solutions were 1, 0.58, 0.50, 0.28, 0.13, and 0.07 for PHF, FOPT-0.5, FOPT-1, FOPT-2, FOPT-4, and FOPT-8, respectively. It is interesting to note that, except for FOPT-0.5, the ϕ_f values scale almost linearly with the amount of phenothiazine/fluorenone incorporated in the terpolymers. These ϕ_f values are factors of 2−4 lower compared to those of corresponding fluorene−fluorenone copolymers that only contained 1−10 mol % of fluorenone moieties.[14d] The presence of the phenothiazine donor moieties in the terpolymers creates additional charge transfer excited states and the associated nonradiative decay channels, resulting in the observed decrease in the PL quantum yields of the terpolymers.

b. Thin Films. The normalized optical absorption spectra of thin films of PHF and the five FOPT terpolymers are shown in Figure 4a. With increasing amounts of fluorenone and phenothiazine, the absorption maximum steadily blue-shifts from 384 nm in PHF to 378 nm in FOPT-8 and the charge transfer absorption band at ~430−500 nm slightly increases. Similar to dilute solution, the low-energy absorption band is very weak

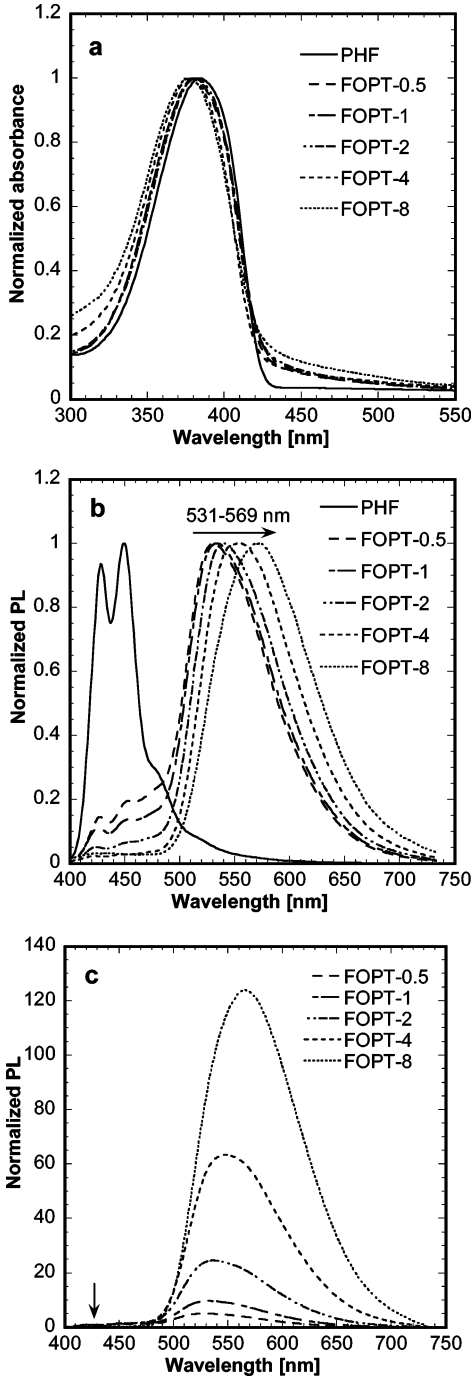

Figure 4. (a) Normalized absorption spectra of thin films of PHF and the five terpolymers. (b) PL emission spectra of polymer thin films normalized relative to their respective dominant peak. (c) PL emission spectra of terpolymer thin films normalized relative to the blue emission at 424 nm. The excitation wavelength was 380 nm.

due to the low concentration of fluorenone in the copolymers and the associated low oscillator strengths. The presence of phenothiazine units is likely manifested in the increased absorption at 300 nm; the phenothiazine homopolymer PHPT had a strong absorption below 300 nm.[12e]

Figure 4b shows the PL emission spectra of the polymer thin films, normalized relative to their respective dominant emission band. The PHF spectrum shows typical blue emission with two distinct peaks at 428 and 449 nm. All the FOPT terpolymer thin films, on the other hand, have significantly red-shifted emission maxima ranging from 531 to 569 nm, thereby emitting green to yellow light. There is additional emission in the 460−490 nm region in the FOPT terpolymer thin films, which was clearly absent in the fluorene−fluorenone copolymer solid-state emission,[14d] suggesting that it is related to the phenothiazine moieties. We note that the two phenothiazine copolymers PHPT and PPTF had their emission maxima at 490 nm in the solid state.[12e] The blue emission is drastically quenched with increasing fluorenone and phenothiazine concentration in the FOPT terpolymers to the extent that it is barely discernible in the emission spectrum of FOPT-4 and FOPT-8 thin films. The reason for this dramatic quenching is the very efficient interchain energy transfer to the low-energy emissive traps due to the increased interchain interactions in the solid state.[14a,b,d,e,19,20] The extent of this quenching in the terpolymers is larger compared to that observed in thin films of fluorene−fluorenone copolymers. For example, the blue emission band was 20% of the intensity of the green band in the copolymer containing only 1 mol % fluorenone (1-FO),[14d] whereas it is only 10% of the intensity of the green band in FOPT-1, which contains 1 mol % of both fluorenone and phenothiazine. Thus, the presence of the phenothiazine moieties in the terpolymers further quenches the blue emission of the fluorene segments.

The solid-state PL emission maxima in these FOPT terpolymers are more red-shifted compared to those of the fluorene−fluorenone copolymers. The lowest-energy emission peak in the terpolymers varies from 531 nm in FOPT-0.5 to 534, 540, 553, and 569 nm for FOPT-1, FOPT-2, FOPT-4, and FOPT-8 thin films, respectively. In comparison, the PL emission maximum in the FO copolymer containing 10 mol % fluorenone (10-FO) was at 546 nm.[14d] Thus, the PL emission peak of FOPT-8, which contains only 8 mol % of both fluorenone and phenothiazine, is red-shifted by 23 nm relative to 10-FO. As mentioned previously, these low-energy emissions are due to charge transfer transitions centered on the fluorenone moieties. In the case of 10-FO, fluorene was the donor component with fluorenone being the acceptor. In the FOPT-8 terpolymer, while the acceptor is still fluorenone, the donor is a combination of both fluorene and phenothiazine. Because of the much stronger electron-donating strength of phenothiazine, the charge transfer emission of FOPT-8 is red-shifted compared to 10-FO.

Figure 4c shows the PL emission spectra of the terpolymer thin films, normalized relative to the blue peak at 424 nm. The ratio of green:blue emission is 5:1, 10:1, 24:1, 63:1, and 124:1, for FOPT-0.5, FOPT-1, FOPT-2, FOPT-4, and FOPT-8, respectively. Similar to the observed variations in the PL quantum yields of the terpolymers in dilute solution, the intensity of the lowest-energy emission in thin films also scales almost linearly with the amount of fluorenone/phenothiazine incorporated in the terpolymers. Compared to the fluorene−fluorenone copolymers, the blue emission is much more quenched in the FOPT terpolymers, particularly in those containing higher fractions of phenothiazine. This is due to the phenothiazine moieties acting as additional energy sinks for the excitation energy on the blue-emitting fluorene segments. The solid-state emission characteristics of the FOPT terpolymers are thus governed by competing intra- and interchain energy transfer processes from the high-energy fluorene segments to two different low-energy emissive traps, viz., fluorene−fluorenone and fluorene−phenothiazine segments.

Time-Resolved PL Decay Dynamics. To further shed light on the excited-state dynamics of the terpolymers, the fluorescence decays of the emission bands were investigated in solutions and thin films of the polymers. The time-resolved PL decay parameters in dilute toluene solution are summarized in Table 2. In dilute toluene solution (10^{-6} M), the decay of the

Table 2. PL Decay Parameters and PL Quantum Yields of the Polymers in 10^{-6} M Toluene Solutions[a]

polymer	λ_{em}[b] (nm)	fit[c]	τ_1 (A_1)[c] ns (%)	τ_2 (A_2)[c] ns (%)	χ^2	DW[d]	ϕ_f (%)
PHF	414	F1	0.360 (100)		1.13	1.75	100
PHPT	472	F1	1.50 (100)		1.18	1.75	
PPTF	485	F1	1.50 (100)		1.00	1.98	
FOPT-0.5	414	F1	0.302 (100)		1.30	1.94	58
	474	F1	0.707 (100)		1.35	1.50	
	520	F2	0.785 (87)	3.67 (13)	0.91	2.17	
FOPT-1	414	F1	0.296 (100)		2.27	1.75	50
	474	F1	0.700 (100)		1.60	1.51	
	520	F2	0.737 (82)	3.42 (18)	0.88	2.00	
FOPT-2	414	F1	0.342 (100)		1.18	1.90	28
	480	F1	1.24 (100)		1.16	1.85	
	520	F2	1.15 (81)	4.12 (19)	1.04	1.93	
FOPT-4	414	F1	0.341 (100)		1.09	1.50	13
	483	F1	1.35 (100)		0.91	1.80	
	523	F2	1.07 (78)	4.67 (22)	1.02	1.91	
FOPT-8	414	F1	0.358 (100)		1.08	2.15	7
	483	F1	1.36 (100)		1.13	1.95	
	524	F2	1.17 (72)	4.93 (28)	0.93	1.95	

[a] Excitation wavelength used = 381 nm. [b] Monitored emission wavelength. [c] F1 = single-exponential fit; F2 = biexponential fit. [c] A_1 and A_2 represent the % amplitude of the lifetime. [d] Durbin−Watson parameter for the fits.

blue emission (414 nm) in the PHF homopolymer and the terpolymers was well-described by a single-exponential fit with short lifetimes ranging from 300 to 360 ps, which matches well with the singlet intrachain exciton lifetimes of polyfluorenes.[21] The FOPT terpolymers had two other (blue-green and green) emission bands in toluene solution (Figure 3b). Figure 5a shows the representative decay curves of FOPT-4 in 10^{-6} M toluene for each of its three emission bands. The blue-green emission (∼475−485 nm) also gave a single-exponential decay with a longer lifetime of 0.7−1.36 ns; the lifetime steadily increased from 0.7 ns in FOPT-0.5 to 1.36 ns in FOPT-8 with increasing phenothiazine and fluorenone content. Identical lifetimes of 1.5 ns were obtained for the blue-green emission of PHPT (472 nm) and PPTF (485 nm). These lifetimes are consistent with the previous assignment of the blue-green emission to the phenothiazine moieties. It appears that the lifetime in the FOPT terpolymers is approaching the 1.5 ns lifetime in PPTF with increasing phenothiazine content from 0.5 to 8 mol %.

The PL decay of the green emission (520−524 nm) of the terpolymers needed two exponentials to obtain acceptable fits; single-exponential fits gave high χ^2 values greater than 4. The dominant component had a relatively short lifetime of ∼0.7−1.2 ns, and the minor component had a longer lifetime of ∼3.4−5.0 ns. In each terpolymer, the shorter lifetime matched fairly well with the lifetime of its blue-green emission, implying that it originates from the phenothiazine moiety. The longer lifetimes are similar to those reported for fluorenone emission in fluorene−fluorenone copolymers;[14d,g] the relative amplitude of this long-lifetime component increases with increasing fluorenone fraction from FOPT-0.5 (13%) to FOPT-8 (28%). These results suggest that the green emission in the terpolymers is a combination of emission from two different sites on the terpolymer chains: the phenothiazine-containing segments and the fluorenone-containing segments. This is depicted in Figure 5b, which shows the steady-state PL emission spectrum of FOPT-4 along with its molecular structure. With excitation at 381 nm, the fluorene segments are selectively excited, and subsequently the excitation hops along the terpolymer chain (within the lifetime of the fluorene excitation) until it finds either the low-energy phenothiazine or fluorenone traps giving rise to the blue-green or green emissions, respectively. As the phenothiazine and fluorenone concentrations in the terpolymer increase, the average distance between the photoexcited fluorene segments and the traps decreases, making the intrachain energy transfer process more efficient. The relative chance of trapping on the fluorenone moieties increases with increasing fluorenone content from FOPT-0.5 to FOPT-8. We note that two very fast components with lifetimes of 10−30 and 70−200 ps were recently reported for fluorene−fluorenone copolymers in toluene solution, and the latter component was assigned to this process of excitation energy migration along the polymer chain.[22] These lifetimes cannot be resolved in our measurements since they are well below the time resolution of our experimental setup.

The PL decay parameters of all the polymer thin films are collected in Table 3. The decay of the blue emission at 426 nm in PHF was single-exponential with a short lifetime of 395 ps. The blue-green emission of PHPT and PPTF had lifetimes of 530 ps and 1.04 ns, respectively, and were also well described by single-exponential kinetics. These lifetimes are shorter than those in solution due to the additional nonradiative channels

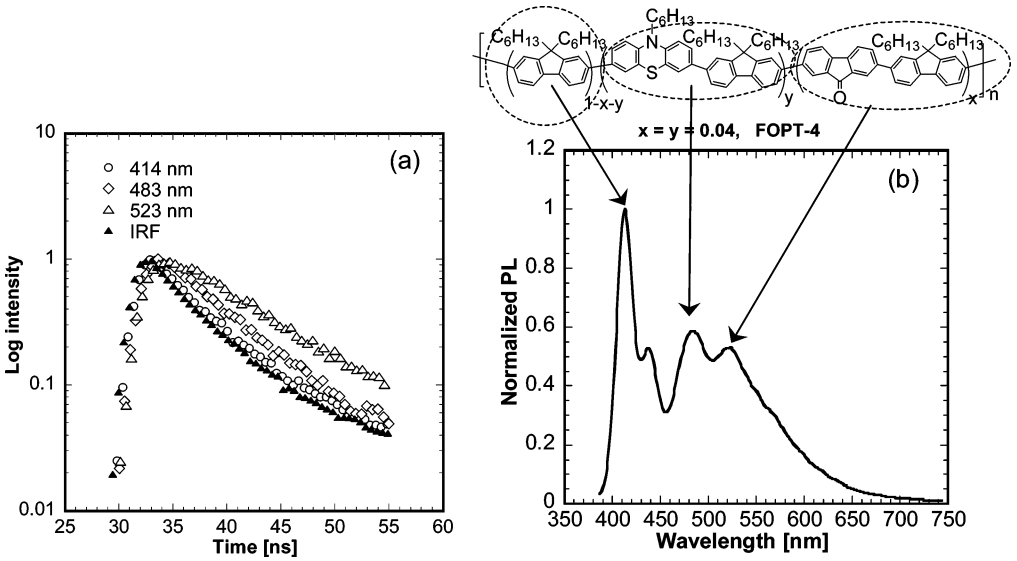

Figure 5. (a) PL decay curves of FOPT-4 in 10^{-6} M toluene solution with 381 nm excitation. IRF denotes the instrument response function. (b) The steady-state PL emission spectrum of FOPT-4 in 10^{-6} M toluene and assignment of the observed three emission bands to the three different conjugated segments (shown by dotted lines) on the terpolymer backbone.

Table 3. PL Decay Parameters of the Polymer Thin Films[a]

polymer	λ_{em}[b] (nm)	τ_1 (A_1)[c] ns (%)	τ_2 (A_2)[c] ns (%)	χ^2	DW[d]
PHF	426	0.395 (100)		1.45	1.60
PHPT	483	0.530 (100)		0.98	2.08
PPTF	490	1.04 (100)		1.15	1.81
FOPT-0.5	527	0.295 (81)	6.49 (19)	1.01	1.87
FOPT-1	532	0.315 (86)	6.58 (14)	1.03	1.92
FOPT-2	536	0.325 (80)	5.40 (20)	1.09	2.02
FOPT-4	547	0.340 (91)	5.96 (9)	1.05	1.77
FOPT-8	565	0.337 (94)	4.77 (6)	1.00	2.14

[a] Excitation wavelength used = 381 nm. [b] Monitored emission wavelength. [c] A_1 and A_2 represent the % amplitude of the lifetime. [d] Durbin−Watson parameter for the fits.

generally encountered in the solid state. In the FOPT terpolymer thin films, the decays of the dominant green-yellow emission bands were well-described by biexponential fits, similar to dilute solution. The dominant component had relatively short lifetimes of less than 350 ps, whereas the minor component had much longer lifetimes of ∼4.8−6.5 ns. Unambiguous assignment of the short-lived component is not trivial; it is likely associated with the transitions centered on the phenothiazine-containing segments. With increasing fluorenone fraction in the terpolymers, the lifetime and the amplitude of the long-lived component decreased from 6.5 ns (19%) in FOPT-0.5 to 4.77 ns (6%) in FOPT-8. This is the exact opposite of the trend observed in dilute toluene solution (Table 2). Given that this long-lived species is associated with the charge transfer transition of the fluorene−fluorenone segments, the decreasing relative amplitudes suggest that energy funneling to the fluorenone units decreases with increasing phenothiazine content in the FOPT terpolymers. Thus, in contrast to the situation in dilute solution, the phenothiazine moieties appear to dominate the emissions in the terpolymer thin films. We note that the PL decays of the low-energy emission bands in all fluorene−fluorenone copolymer thin films were well-described by single-exponential fits,[14d] implying the presence of only one type of emitting species, viz., the charge transfer excited state of fluorenone. The incorporation of phenothiazine moieties in the terpolymers leads to additional pathways for excited-state depopulation which compete with the fluorenone moieties for the excitation energy.

Electroluminescence. Figure 6 shows the electroluminescence (EL) spectra, normalized relative to the blue emission band (420−424 nm), of single-layer OLEDs of the type ITO/PEDOT/terpolymer/LiF/Al based on the five terpolymers. The EL spectra of all the terpolymers are very dependent on the applied voltage. For example, consider the EL spectra of FOPT-1 shown in Figure 6b which have two emission bands, a blue band at 421 nm and a green band at 527−531 nm, whose positions match well with the thin film PL emission (Figure 4b). At the lowest voltage (6.0 V), the green peak (531 nm) is 1.5 times the intensity of the blue peak. At 8.0 V, the green peak increases to nearly 8 times the intensity of the blue peak. At higher voltages (>8 V), the green peak steadily gets suppressed; the green:blue intensity decreases from 6.5 to 5 to 4.3 with increasing voltage from 9 to 10 to 11 V, respectively. A similar variation in the green:blue EL intensity with voltage is observed in the EL spectra of the other terpolymers. The blue band gets significantly quenched with increasing phenothiazine and fluorenone content, as seen in parts c−e of Figure 6. The green:blue emission ratio in EL of the terpolymers exceeds that in PL for FOPT-0.5, FOPT-2, and FOPT-4. In the case of FOPT-1 and FOPT-8, however, the maximum green:blue emission ratio in EL is lower than that seen in their thin film PL emission.

The variation in the green:blue EL ratio as a function of the applied electric field is shown in Figure 6f for the five terpolymers. In general, the emission ratio increases with increasing fluorenone and phenothiazine content in the terpolymers. In each terpolymer, a steady increase in the green:blue emission ratio with electric field is observed up to a point, above which there is saturation and subsequent decrease with increasing field strength. The electric field at which the above transition occurs varies with the terpolymer composition. In FOPT-0.5 and FOPT-2, the transition field is ∼1.4 MV/cm; in FOPT-1, FOPT-4, and FOPT-8, it is ∼2−2.2 MV/cm. This decrease in the green:blue ratio at higher voltages is in contrast to the trend previously observed in fluorene-fluorenone copolymers where the green:blue EL ratio steadily increased with increasing voltage (electric field) up to the maximum operating voltage.[14d] The extent of decrease in the green:blue ratio increases with increasing phenothiazine/fluorenone content in the terpolymer. For example, in FOPT-0.5, the ratio varies from a maximum value of 9.8 (at 1.4 MV/cm) to 4.3 (at 2.4 MV/cm) at the highest electric field, corresponding to a decrease by 56%. On the other hand, in FOPT-4, the ratio decreases from a maximum value of 167 (at 2.0 MV/cm) to 31 (at 2.9 MV/cm), corresponding to a drop of 81%.

To understand the reasons for this variation in the green:blue EL ratio, we need to consider the electronic structure of the terpolymers. Previous experimental and theoretical studies have shown that phenothiazine (HPT) and fluorenone (FLO) moieties act as hole and electron traps on poly(9,9-dihexylfluorene) (PHF) chains, respectively.[12,13,23] The depth of the traps and the radiative recombination efficiency on each emissive trap will determine the ratio of the blue fluorene emission to the low-energy trap emission. Such charge-trapping and recombination dynamics are known to depend on the electric field.[24] Figure 7 shows a schematic energy level diagram for the terpolymers, indicating the HOMO/LUMO levels corresponding to the parent PHF backbone and the HPT and FLO traps that are isolated within the PHF chains. The higher-lying HOMO level of HPT (5.0 eV) relative to that of PHF (5.6 eV) results in a hole trap with a depth of 0.6 eV. The lower-lying LUMO level of FLO (3.1 eV) compared to that of PHF (2.5 eV) constitutes a 0.6 eV deep electron trap. The variation in the green:blue ratio with electric field shown in Figure 6f points to two distinct regimes: a low field regime where the ratio increases with increasing field and a high field regime where the ratio decreases with increasing field strength. At the low fields, electron trapping on FLO moieties appears to dominate; radiative recombination on the FLO moieties between the trapped electrons and mobile holes on the PHF backbone would explain the observed initial increase in the green:blue ratio in each terpolymer. At the higher fields, hole trapping on the HPT moieties begins to dominate, making fewer holes available for recombination on the FLO traps. The probability of these trapped holes to recombine with mobile electrons on the blue-emitting fluorene segments increases, resulting in a decrease in the green:blue EL ratio at the high electric fields. This hole trapping effect should become more dominant with increasing HPT content in the terpolymer, explaining the observed larger drop in the green:blue ratio in FOPT-4 compared to FOPT-0.5. The absence of the phenothiazine moieties in the previously reported fluorene−fluorenone copolymers is a plausible reason why no such decrease in the green:blue EL ratio was observed even at the highest electric fields in those copolymer diodes.[14d]

The current density−electric field and luminance−voltage characteristics of the single-layer terpolymer diodes are shown

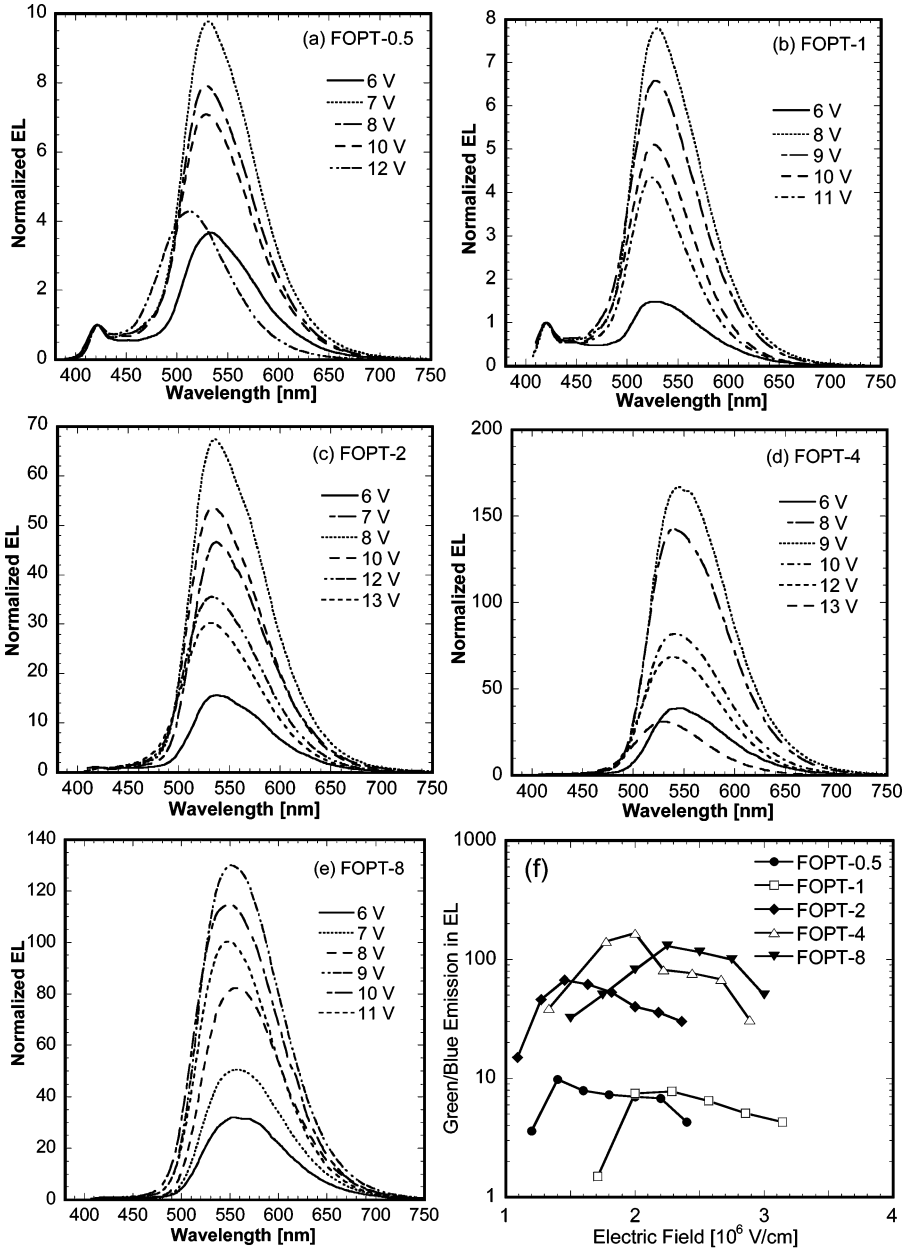

Figure 6. Normailzed EL spectra of single-layer diodes of the type ITO/PEDOT/terpolymer/LiF/Al: (a) FOPT-0.5, (b) FOPT-1, (c) FOPT-2, (d) FOPT-4, and (e) FOPT-8. (f) Variation in the green:blue EL emission ratio vs electric field.

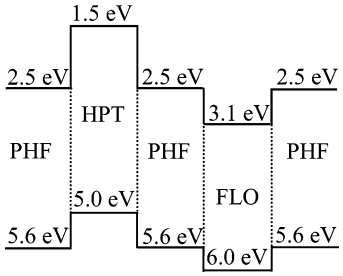

Figure 7. Schematic energy level diagram for FOPT terpolymers. The energy levels of PHF are taken from ref 5c. The HOMO level of HPT is taken from ref 12b; the LUMO level is estimated from the absorption spectrum of HPT and using LUMO = optical band gap − HOMO. The LUMO level of FLO is taken from ref 14f; its HOMO level is approximated using optical band gap value of 2.9 eV from the absorption spectrum of FLO.

in Figure 8, parts a and b, respectively. At the same electric fields, the currents passing through the terpolymer devices generally decrease with increasing fluorenone/phenothiazine content, suggesting higher charge (electron/hole) trapping and better charge recombination efficiency. FOPT-1 devices have the lowest current densities, for reasons that are not obvious. The variation in the brightness of the LEDs as a function of applied voltage is shown in Figure 8b. The brightness varied with terpolymer composition; the maximum luminance was 1435, 655, 2250, 930, and 460 cd/m^2 for the FOPT-0.5, FOPT-1, FOPT-2, FOPT-4, and FOPT-8 diodes, respectively. Thus, FOPT-2 devices were brightest whereas the smallest maximum brightness was obtained in the FOPT-8 diode. The corresponding maximum luminous efficiencies were 0.33, 0.14, 0.51, 0.22, and 0.10 cd/A. For comparison, the dilute solution PL quantum yields of the corresponding copolymers were 0.58, 0.50, 0.28, 0.13, and 0.07 (Table 2). Thus, although FOPT-2 has a factor of 2 lower PL quantum yield than FOPT-0.5 and FOPT-1, the FOPT-2 devices have better performance than those from the latter copolymers. It appears that 2 mol % phenothiazine and fluorenone is the optimum terpolymer composition for balanced charge injection and transport and charge recombination. The

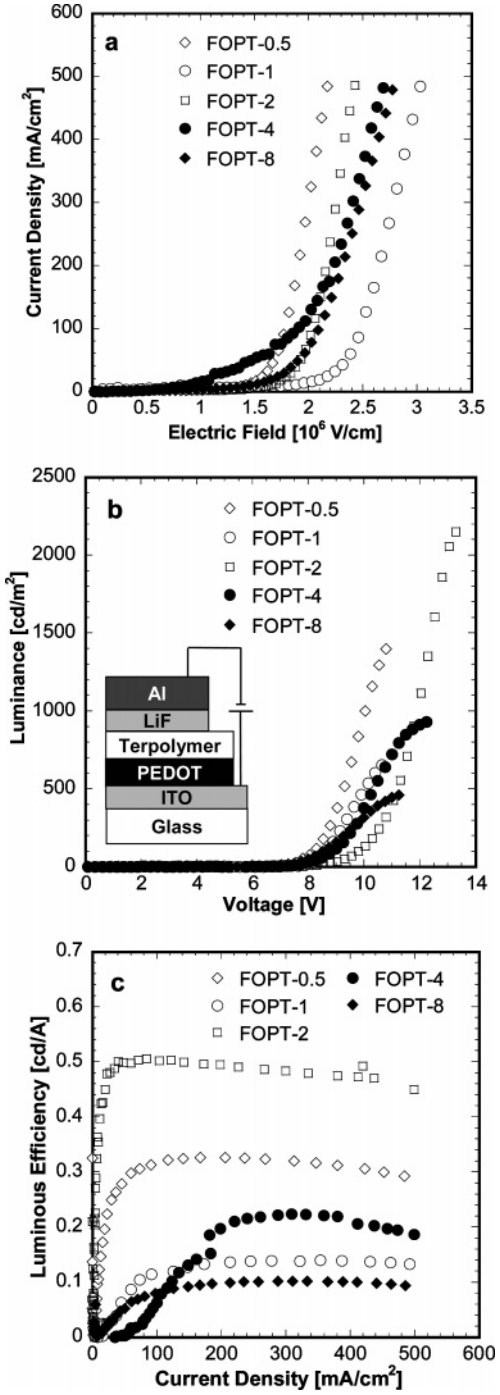

Figure 8. (a) Current density−electric field characteristics of single-layer terpolymer LEDs. (b) Luminance−voltage characteristics of the devices in (a) and the inset shows the device schematic. (c) Luminous efficiency as a function of the current density of the devices.

device characteristics of the five terpolymers are summarized in Table 4.

Figure 8c shows the variation in the luminous efficiency of the single-layer devices vs current density for all the terpolymers. The efficiencies remain fairly constant over a wide current density range from ~100−500 mA/cm^2 in all terpolymers, except FOPT-4. It is clear that FOPT-2 gives the superior device performance among the five copolymers. FOPT-1 devices have an efficiency lower than the FOPT-4 diodes, especially at the high current densities (>180 mA/cm^2), for reasons that are not clear. Overall, we note that the maximum brightnesses and efficiencies obtained with these terpolymers are lower compared

Table 4. Device Characteristics of Terpolymer OLEDs

polymer	device structure[a]	max brightness, cd/m^2 (V, cd/A)	max efficiency, cd/A (V, cd/m^2)	1931 CIE (x, y)[b]
FOPT-0.5	1	1435 (11.0, 0.28)	0.33 (9.5, 640)	(0.30, 0.55)
	2	2525 (12.0, 0.50)	0.61 (8.9, 270)	(0.31, 0.54)
	3	7100 (11.3, 1.41)	2.95 (8.1, 1295)	(0.28, 0.47)
FOPT-1	1	655 (10.7, 0.13)	0.14 (10.0, 355)	(0.28, 0.55)
	2	1175 (11.0, 0.23)	0.28 (9.0, 300)	(0.33, 0.56)
	3	4120 (12.0, 0.82)	0.82 (12.0, 4120)	(0.30, 0.50)
FOPT-2	1	2250 (13.4, 0.45)	0.51 (11.0, 425)	(0.35, 0.58)
	2	3270 (13.5, 0.67)	0.79 (12.5, 2255)	(0.35, 0.58)
	3	8975 (12.8, 2.48)	3.40 (10.2, 1255)	(0.34, 0.57)
FOPT-4	1	930 (12.3, 0.19)	0.22 (10.9, 690)	(0.38, 0.58)
	2	1520 (12.5, 0.30)	0.36 (9.4, 195)	(0.39, 0.57)
	3	5220 (12.5, 1.04)	1.56 (9.0, 810)	(0.38, 0.56)
FOPT-8	1	460 (11.3, 0.09)	0.10 (10.1, 330)	(0.40, 0.56)
	2	675 (11.2, 0.13)	0.19 (9.0, 110)	(0.42, 0.55)
	3	1890 (11.2, 0.40)	0.55 (8.7, 550)	(0.40, 0.55)

[a] Device structures: (1) ITO/PEDOT/polymer/LiF/Al; (2) ITO/PEDOT/PVK/polymer/LiF/Al; (3) ITO/PEDOT/PVK/polymer/TPBI/LiF/Al. [b] CIE coordinates at maximum device efficiency.

to those reported previously for similar fluorene−fluorenone copolymer devices.[14d] The much lower PL quantum yields of the terpolymers can explain the observed differences in device performance. Thus, while the hole-injection and transport properties of the terpolymers are improved by the incorporation of the donor phenothiazine moieties, these come at the expense of the reduced PL emission efficiencies, resulting ultimately in lower EL efficiencies. These results demonstrate that to attain the perfect balance between hole and electron injection/transport and the desired high EL efficiency in multichromophore copolymers, the choice of the D and A moieties and their relative ratios need careful consideration, since the efficiency of energy and intrachain charge transfer processes depends critically on that choice.

One of the central themes in this paper concerns the variation in the charge trapping dynamics[25] (the green:blue EL emission ratio) and the associated competing energy transfer processes with electric field in devices based on D/A-containing polyfluorenes. To further investigate the effect of changing the hole/electron injection and transport characteristics in the devices on the green:blue EL emission ratio, we fabricated two more sets of terpolymer devices: one with a PVK hole-transport/electron-blocking layer (IP = 5.8 eV, EA = 2.3 eV)[2d] and the other with a TPBI electron-transport/hole-blocking layer (IP = 6.2−6.7 eV, EA = 2.7 eV).[1d] The previous finding that addition of a PVK layer reduces the green EL emission in fluorenone−fluorene copolymers[26] partly motivated these studies, in addition to the fact these additional layers of PVK and TPBI should presumably lead to better device performances than the single-layer diodes.

Figure 9, parts a and b, shows the variation in the green:blue EL emission ratio as a function of the electric field for the bilayer and trilayer devices, respectively. These results are to be compared with the corresponding results for the single-layer devices (Figure 6f). We note that emission from either the PVK or TPBI layer was not observed in the respective EL spectra of the terpolymer devices (not shown). Upon incorporation of a 20 nm thick PVK layer, the green:blue emission ratios are enhanced in all the terpolymers, particularly at the low electric fields <1.5 MV/cm (Figure 9a). Since electron trapping on the fluorenone moieties appears to dominate at the low electric fields, the increase in the density of available holes upon incorporation of PVK layer results in higher radiative recombination on the fluorenone moieties and enhanced green emission. At the higher electric fields, the emission ratios

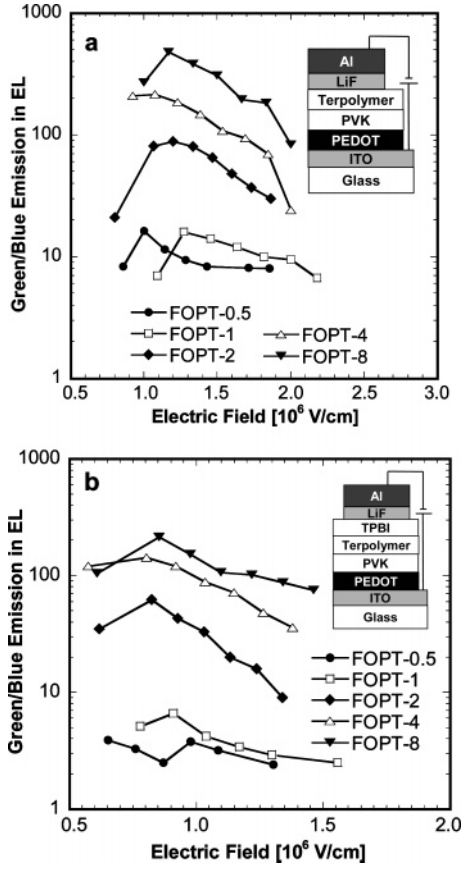

Figure 9. Variation in the green:blue EL emission ratio vs electric field for bilayer (a) and trilayer (b) terpolymer diodes. The inset shows the device schematic.

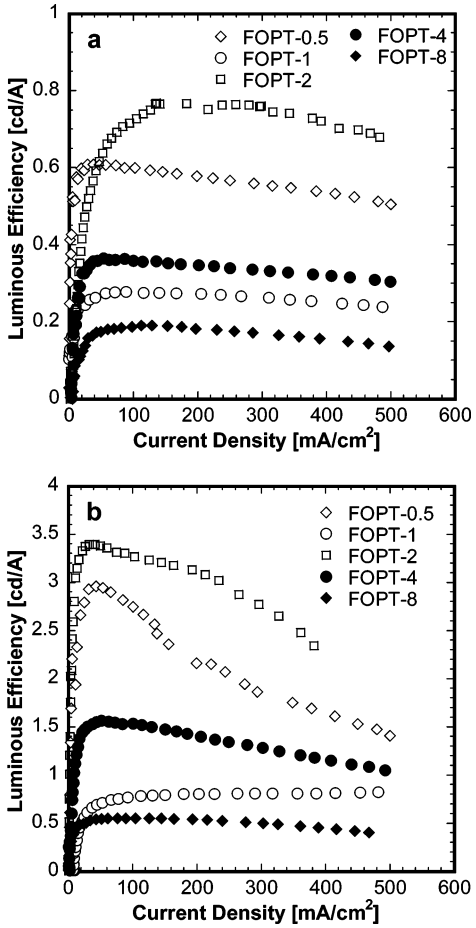

Figure 10. Luminous efficiency as a function of the current density of terpolymer diodes: (a) bilayer PVK/terpolymer devices and (b) trilayer PVK/terpolymer/TPBI devices.

decrease rapidly to become comparable to those observed in the single-layer devices at their maximum electric fields. When a 20 nm thick TPBI layer is added (Figure 9b), the green:blue emission ratios are significantly reduced in all five terpolymers compared to their bilayer devices. In fact, the emission ratio in the FOPT-0.5, FOPT-1, and FOPT-2 trilayer diodes is even lower compared to their single-layer devices over the entire range of electric fields. The TPBI layer would not only increase the density of free electrons in the device but also likely enhance the hole-trapping effect on the phenothiazine moieties due to its hole-blocking capability. Both processes would lead to a higher probability of radiative recombination on the blue-emitting fluorene segments, explaining the observed reduction in the green:blue EL ratio in the trilayer devices.

To understand the implications of the observed variations in the green:blue emission ratio with applied voltage on the EL properties of the terpolymer devices (Figures 6f and 9), one has to consider the extent of change in the emission CIE coordinates over the entire operating voltage range. Let us consider the single-layer device based on FOPT-1 (Figure 6b). The green:blue EL ratio increased from 1.5 (at 6 V) to 7.9 (at 8.0 V) and then decreased to 4.3 (at 11 V). The corresponding CIE coordinates were (0.28, 0.43) at 6 V, (0.31, 0.56) at 8 V, and (0.27, 0.54) at 11 V. This represents a perceptible change in the EL emission colors with voltage, although they all fall within the yellowish-green region. In the case of FOPT-8 (Figure 6e), the green:blue EL ratio varied from 32 (at 6 V) up to 130 (at 9 V) and down to 100 (at 11 V). The corresponding CIE coordinates were (0.43, 0.53) at 6 V, (0.42, 0.55) at 9 V, and (0.40, 0.55) at 11 V. Here, despite the significant variation in the ratio, the CIE coordinates of the EL emission remain similar over the entire operating voltage range. Since the relative contribution of the blue emission band is small (<5%) in the FOPT-2, FOPT-4, and FOPT-8 terpolymers, the variation in the green:blue ratio does not significantly affect their EL emission color quality. However, in FOPT-0.5 and FOPT-1 terpolymers containing low amounts (≤ 1 mol %) of phenothiazine and fluorenone, there is appreciable change in the emission CIE coordinates with drive voltage. These results are important in light of the fact that multichromophore copolymers that are being developed for single-layer white OLEDs typically have very small amounts (≪1 mol %) of green- and orange/red-emitting D/A comonomers incorporated into the blue-emitting backbone.[9] An analysis of the charge-trapping dynamics and associated energy transfer processes of the kind presented here is critical to developing an understanding of the main factors leading to a voltage-independent white EL, which has been challenging to achieve so far in such multichromophoric copolymers.

Finally, the variation in the luminous efficiency of the bilayer and trilayer terpolymer devices is shown in Figure 10, parts a and b, respectively. As expected, the efficiencies are enhanced upon incorporation of the PVK and TPBI layers, compared to those obtained in the single-layer diodes (Figure 8c), due to the improved charge balance and recombination in the multilayered devices. The efficiencies are fairly constant over a wide range of current densities in most devices, suggesting balanced charge injection and recombination efficiency over the entire operating voltage range. The relative trend in efficiency among the terpolymers remains the same as in the single-layer diodes;

FOPT-2 and FOPT-8 give the highest and lowest device performances, respectively. As summarized in Table 4, the brightnesses of all the terpolymer LEDs increase by factors of 1.5−1.7 and the maximum efficiencies increase by factors of 1.5−2.0 by going from the single-layer to the bilayer device architecture. Much better improvements in brightness by factors of 4−6 and efficiencies by factors of 5.5−9.0 are achieved in going from the single layer to the trilayer devices. A maximum brightness of 8975 cd/m^2 and a maximum efficiency of 3.4 cd/A at 1255 cd/m^2 with green CIE coordinates of $x = 0.34$, $y = 0.57$ were obtained from the trilayer devices based on FOPT-2. Given the extent of enhancement observed in the device performance in the current terpolymers in going from the simple single-layer to the trilayer geometry, a similar exercise with the fluorene−fluorenone copolymers[14d] should lead to high brightness and efficiency green polymer LEDs based on them.

Conclusions

We have synthesized five new poly(9,9-dihexylfluorene) terpolymers containing 0.5, 1, 2, 4, and 8 mol % each of electron-rich 10-hexylphenothiazine and electron-deficient 9-fluorenone moieties and used them to investigate the effects of intrachain excited-state dynamics on the photophysics and electroluminescence of multichromophore copolymers. We found that the PL and EL emission characteristics of the terpolymers are governed by competing intra- and interchain energy transfer processes from the high-energy fluorene segments to the two low-energy emissive traps associated with fluorene−phenothiazine and fluorene−fluorenone chain segments. The presence of the phenothiazine moieties created additional charge transfer excited states and associated nonradiative decay channels, resulting in the factors of 2−4 decrease in the PL quantum yields of the fluorene−phenothiazine−fluorenone terpolymers and a higher degree of quenching of the blue emission compared to previous fluorene−fluorenone copolymers. The excited-state dynamics varies in going from dilute solution to thin film, where the three-dimensional nature of the energy migration and transfer processes significantly suppresses the blue emission. Green to yellow EL was achieved from the terpolymer light-emitting devices with luminances of 1900−8970 cd/m^2 and efficiencies of 0.5−3.5 cd/A that varied with copolymer composition. Since the phenothiazine and fluorenone moieties also act as charge carrier traps under electrical excitation, the EL spectra were highly dependent on the applied voltage, the terpolymer composition, and device architecture due to the dependence of the charge-trapping dynamics on the electric field. These results reveal that the excited-state dynamics encountered in electroluminescent, multichromophore copolymers being developed for white LEDs can be very complex and thus must be duly taken into account in the design of materials.

Acknowledgment. We acknowledge support from the NSF STC MDITR (DMR-0120967), the NSF (CTS-0437912), and the Air Force Office of Scientific Research (Grant F49620-03-1-0162).

References and Notes

(1) Reviews on polymer electroluminescence: (a) Bernius, M. T.; Inbasekaran, M.; O'Brien, J.; Wu, W. *Adv. Mater.* **2000**, *12*, 1737−1750. (b) Kraft, A.; Grimsdale, A. C.; Holmes, A. B. *Angew. Chem., Int. Ed.* **1998**, *37*, 402−428. (c) Kim, D. Y.; Cho, H. N.; Kim, C. Y. *Prog. Polym. Sci.* **2000**, *25*, 1089−1139. (d) Kulkarni, A. P.; Tonzola, C. J.; Babel, A.; Jenekhe, S. A. *Chem. Mater.* **2004**, *16*, 4556−4573 and references therein.

(2) (a) Cirpan, A.; Ding, L.; Karasz, F. E. *Synth. Met.* **2005**, *150*, 195−198. (b) Peng, Z.; Bao, Z.; Galvin, M. E. *Chem. Mater.* **1998**, *10*, 2086−2090. (c) Tarkka, R. M.; Zhang, X.; Jenekhe, S. A. *J. Am. Chem. Soc.* **1996**, *118*, 9438−9439. (d) Zhang, X.; Shetty, A. S.; Jenekhe, S. A. *Macromolecules* **1999**, *32*, 7422−7429. (e) Zhang, X.; Jenekhe, S. A. *Macromolecules* **2000**, *33*, 2069−2082. (f) Tonzola, C. J.; Alam, M. M.; Jenekhe, S. A. *Adv. Mater.* **2002**, *14*, 1086−1090.

(3) (a) Cornil, J.; Gueli, I.; Dkhissi, A.; Sancho-Garcia, J. C.; Hennebicq, E.; Calbert, J. P.; Lemaur, V.; Beljonne, D.; Bredas, J.-L. *J. Chem. Phys.* **2003**, *118*, 6615−6623. (b) Jenekhe, S. A.; Osaheni, J. A. *Science* **1994**, *265*, 765−768.

(4) Reviews on polyfluorenes: (a) Neher, D. *Macromol. Rapid Commun.* **2001**, *22*, 1365−1385. (b) Scherf, U.; List, E. J. W. *Adv. Mater.* **2002**, *14*, 477−487. (c) Leclerc, M. *J. Polym. Sci., Part A: Polym. Chem.* **2001**, *39*, 2867−2873. (d) Becker, S.; Ego, C.; Grimsdale, A. C.; List, E. J. W.; Marsitzky, D.; Pogantsch, A.; Setayesh, S.; Leising, G.; Müllen, K. *Synth. Met.* **2002**, *125*, 73−80. (e) Chen, P.; Yang, G.; Liu, T.; Li, T.; Wang, M.; Huang, W. *Polym. Int.* **2006**, *55*, 473−490.

(5) (a) Millard, I. S. *Synth. Met.* **2000**, *111*−*112*, 119−123. (b) Wu, W.; Inbasekaran, M.; Hudack, M.; Welsh, D.; Yu, W.; Cheng, Y.; Wang, C.; Kram, S.; Tacey, M.; Bernius, M.; Fletcher, R.; Kiszka, K.; Munger, S.; O'Brien, J. *Microelectron. J.* **2004**, *35*, 343−348. (c) Liao, L. S.; Fung, M. K.; Lee, C. S.; Lee, S. T.; Inbasekaran, M.; Woo, E. P.; Wu, W. W. *Appl. Phys. Lett.* **2000**, *76*, 3582−3584.

(6) (a) Sainova, D.; Miteva, T.; Nothofer, G.; Scherf, U.; Glowacki, I.; Ulanski, J.; Fujikawa, H.; Neher, D. *Appl. Phys. Lett.* **2000**, *76*, 1810−1812. (b) Weinfurtner, K.-H.; Fujikawa, H.; Tokito, S.; Taga, Y. *Appl. Phys. Lett.* **2000**, *76*, 2502−2504. (c) Kulkarni, A. P.; Jenekhe, S. A. *Macromolecules* **2003**, *36*, 5285−5296.

(7) (a) Hung, M.-C.; Liao, J.-L.; Chen, S.-A.; Chen, S.-H.; Su, A.-C. *J. Am. Chem. Soc.* **2005**, *127*, 14576−14577. (b) Li, J. Y.; Ziegler, A.; Wegner, G. *Chem.—Eur. J.* **2005**, *11*, 4450−4457. (c) Xin, Y.; Wen, G.-A.; Zeng, W.-J.; Zhao, L.; Zhu, X.-R.; Fan, Q.-L.; Feng, J.-C.; Wang, L.-H.; Wei, W.; Peng, B.; Cao, Y.; Huang, W. *Macromolecules* **2005**, *38*, 6755−6758. (d) Zhan, X.; Liu, Y.; Wu, X.; Wang, S.; Zhu, D. *Macromolecules* **2002**, *35*, 2529−2537. (e) Shu, C.-F.; Dodda, R.; Wu, F.-I.; Liu, M. S.; Jen, A. K.-Y. *Macromolecules* **2003**, *36*, 6698−6703. (f) Kulkarni, A. P.; Zhu, Y.; Jenekhe, S. A. *Macromolecules* **2005**, *38*, 1553−1563.

(8) (a) Muller, C. D.; Falcou, A.; Reckefuss, N.; Rojahn, M.; Wiederhirn, V.; Rudati, P.; Frohne, H.; Nuyken, O.; Becker, H.; Meerholz, K. *Nature (London)* **2003**, *421*, 829−833. (b) Herguth, P.; Jiang, X.; Liu, M. S.; Jen, A. K.-Y. *Macromolecules* **2002**, *35*, 6094−6100. (c) Wu, W.-C.; Liu, C.-L.; Chen, W.-C. *Polymer* **2006**, *47*, 527−538. (d) Beaupre, S.; Leclerc, M. *Adv. Funct. Mater.* **2002**, *12*, 192−196. (e) Yang, R.; Tian, R.; Yan, J.; Zhang, Y.; Yang, J.; Hou, Q.; Yang, W.; Zhang, C.; Cao, Y. *Macromolecules* **2005**, *38*, 244−253.

(9) (a) Buchhauser, D.; Scheffel, M.; Rogler, W.; Tschamber, C.; Heuser, K.; Hunze, A.; Gieres, G.; Henseler, D.; Jakowetz, W.; Diekmann, K.; Winnacker, A.; Becker, H.; Buesing, A.; Falcou, A.; Rau, L.; Voegele, S.; Goettling, S. *Proc. SPIE* **2004**, *5519*, 70−81. (b) Liu, J.; Zhou, Q.; Cheng, Y.; Geng, Y.; Wang, L.; Ma, D.; Jing, X.; Wang, F. *Adv. Mater.* **2005**, *17*, 2974−2978. (c) Liu, J.; Zhou, Q.; Cheng, Y.; Geng, Y.; Wang, L.; Ma, D.; Jing, X.; Wang, F. *Adv. Funct. Mater.* **2006**, *16*, 957−965. (d) Wu, W.-C.; Lee, W.-Y.; Chen, W.-C. *Macromol. Chem. Phys.* **2006**, *207*, 1131−1138.

(10) (a) Zhang, F.; Perzon, E.; Wang, X.; Mammo, W.; Andersson, M. R.; Inganas, O. *Adv. Funct. Mater.* **2005**, *15*, 745−750. (b) Brabec, C. J.; Winder, C.; Sariciftci, N. S.; Hummelen, J. C.; Dhanabalan, A.; Van Hal, P. A.; Janssen, R. A. J. *Adv. Funct. Mater.* **2002**, *12*, 709−712. (c) Winder, C.; Sariciftci, N. S. *J. Mater. Chem.* **2004**, *14*, 1077−1086.

(11) (a) Champion, R. D.; Cheng, K.-F.; Pai, C.-L.; Chen, W.-C.; Jenekhe, S. A. *Macromol. Rapid Commun.* **2005**, *26*, 1835−1840. (b) Yamamoto, T.; Yasuda, T.; Sakai, Y.; Aramaki, S. *Macromol. Rapid Commun.* **2005**, *26*, 1214−1217.

(12) (a) Jenekhe, S. A.; Lu, L.; Alam, M. M. *Macromolecules* **2001**, *34*, 7315−7324. (b) Kulkarni, A. P.; Wu, P.-T.; Kwon, T. W.; Jenekhe, S. A. *J. Phys. Chem. B* **2005**, *109*, 19584−19594. (c) Zhu, Y.; Kulkarni, A. P.; Jenekhe, S. A. *Chem. Mater.* **2005**, *17*, 5225−5227. (d) Kulkarni, A. P.; Kong, X.; Jenekhe, S. A. *Adv. Funct. Mater.* **2006**, *16*, 1057−1066. (e) Kong, X.; Kulkarni, A. P.; Jenekhe, S. A. *Macromolecules* **2003**, *36*, 8992−8999. (f) Hwang, D.-H.; Kim, S.-K.; Park, M.-J.; Lee, J.-H.; Koo, B.-W.; Kang, I.-N.; Kim, S.-H.; Zyung, T. *Chem. Mater.* **2004**, *16*, 1298−1303. (g) Cho, N. S.; Park, J.-H.; Lee, S.-K.; Lee, J.; Shim, H.-K.; Park, M.-J.; Hwang, D.-H.; Jung, B.-J. *Macromolecules* **2006**, *39*, 177−183. (h) Hancock, J. M.; Gifford, A. P.; Zhu, Y.; Lou, Y.; Jenekhe, S. A. *Chem. Mater.* **2006**, *18*, 4924−4932.

(13) (a) Zojer, E.; Pogantsch, A.; Hennebicq, E.; Beljonne, D.; Brédas, J.-L.; Scanducci de Freitas, P.; Scherf, U.; List, E. J. W. *J. Chem.*

Phys. **2002**, *117*, 6794−6802. (b) Franco, I.; Tretiak, S. *Chem. Phys. Lett.* **2003**, *372*, 403−408.

(14) (a) List, E. J. W.; Guentner, R.; Scanducci de Freitas, P.; Scherf, U. *Adv. Mater.* **2002**, *14*, 374−378. (b) Lupton, J. M.; Craig, M. R.; Meijer, E. W. *Appl. Phys. Lett.* **2002**, *80*, 4489−4491. (c) Gong, X.; Iyer, P. K.; Moses, D.; Bazan, G. C.; Heeger, A. J.; Xiao, S. S. *Adv. Funct. Mater.* **2003**, *13*, 325−330. (d) Kulkarni, A. P.; Kong, X.; Jenekhe, S. A. *J. Phys. Chem. B* **2004**, *108*, 8689−8701. (e) Sims, M.; Bradley, D. D. C.; Ariu, M.; Koeberg, M.; Asimakis, A.; Grell, M.; Lidzey, D. G. *Adv. Funct. Mater.* **2004**, *14*, 765−781. (f) Chi, C.; Im, C.; Enkelmann, V.; Ziegler, A.; Lieser, G.; Wegner, G. *Chem.*−*Eur. J.* **2005**, *11*, 6833−6845. (g) Dias, F. B.; Maiti, M.; Hintschich, S. I.; Monkman, A. P. *J. Chem. Phys.* **2005**, *122*, 054904-1−054904-11.

(15) Kramer, C. S.; Zimmermann, T. J.; Sailer, M.; Muller, T. J. J. *Synthesis* **2002**, 1163−1170.

(16) Heinrich, G.; Schoof, S.; Gusten, H. *J. Photochem.* **1974**, *3*, 315−320.

(17) Reichardt, C. *Solvents and Solvent Effects in Organic Chemistry*; Verlag Chemie: New York, 1988.

(18) Redecker, M.; Bradley, D. D. C.; Baldwin, K. J.; Smith, D. A.; Inbasekaran, M.; Wu, W. W.; Woo, E. P. *J. Mater. Chem.* **1999**, *9*, 2151−2154.

(19) (a) Guillet, J. *Polymer Photophysics and Photochemistry*; Cambridge University Press: Cambridge, 1985; Chapter 9. (b) List, E. J. W.; Creely, C.; Leising, G.; Schulte, N.; Schluter, A. D.; Scherf, U.; Mullen, K.; Graupner, W. *Chem. Phys. Lett.* **2000**, *325*, 132−138.

(20) (a) Cornil, J.; Beljonne, D.; Calbert, J.-P.; Bredas, J.-L. *Adv. Mater.* **2001**, *13*, 1053−1067. (b) Bredas, J.-L.; Beljonne, D.; Coropceanu, V.; Cornil, J. *Chem. Rev.* **2004**, *104*, 4971−5003.

(21) Teetsov, J.; Fox, M. A. *J. Mater. Chem.* **1999**, *9*, 2117−2122.

(22) Dias, F. B.; Knaapila, M.; Monkman, A. P.; Burrows, H. D. *Macromolecules* **2006**, *39*, 1598−1606.

(23) Yang, L.; Feng, J.-K.; Ren, A.-M. *J. Org. Chem.* **2005**, *70*, 5987−5996.

(24) (a) Lupton, J. M.; Klein, J. *Phys. Rev. B* **2002**, *65*, 193202-1−193202-4. (b) Nikitenko, V. R.; Lupton, J. M. *J. Appl. Phys.* **2003**, *93*, 5973−5977.

(25) (a) Kadashchuk, A.; Schmechel, R.; von Seggern, H.; Scherf, U.; Vakhnin, A. *J. Appl. Phys.* **2005**, *98*, 024101-1−024101-8. (b) Konezny, S. J.; Smith, D. L.; Galvin, M. E.; Rothberg, L. J. *J. Appl. Phys.* **2006**, *99*, 064509-1−064509-12.

(26) Yang, X. H.; Jaiser, F.; Neher, D.; Lawson, P. V.; Bredas, J.-L.; Zojer, E.; Guentner, R.; Scanduicci de Freitas, P.; Forster, M.; Scherf, U. *Adv. Funct. Mater.* **2004**, *14*, 1097−1104.

MA0617062